Paper:

Discrimination of Vascular Conditions Using a Probabilistic Neural Network

Akira Sakane*, Toshio Tsuji*, Noboru Saeki, and Masashi Kawamoto****

*Graduate School of Engineering, Hiroshima University
1-4-1 Kagamiyama, Higashi-Hiroshima, Hiroshima 739-8527, Japan
**Graduate School of Biomedical Sciences, Hiroshima University
1-2-3 Kasumi, Minami-ku, Hiroshima 734-8551, Japan
E-mail: sakane@bsys.hiroshima-u.ac.jp
[Received October 20, 2003; accepted December 5, 2003]

This paper proposes a new method to discriminate vascular conditions from changes of biological signals and arterial wall impedance using a neural network. Since strong individual differences cause difficulty in discriminating the vascular conditions, we introduce an impedance ratio of the arterial wall and attempt to discriminate the vascular conditions during surgical operations. From experimental results, it is shown that various stimulations during operations cause changes in the impedance parameters of the arterial wall, and vascular conditions such as vasodilation, vasoconstriction, and shock can be discriminated accurately using the proposed method. This method will be useful for monitoring the vascular conditions during operations.

Keywords: neural network, arterial wall impedance, vascular conditions, impedance ratio

1. Introduction

Physician must accurately determine patients' condition to take proper steps in surgery and emergency treatment. Electrocardiogram (ECG) and arterial pressure are among the biological signals physicians use to diagnose patients. Changes observed in time-domain waveforms can be used to monitor blood circulation to organs and tissues [1], but physicians must have expert knowledge and sufficient experience to catch subtle changes in waveforms, infer causes, and make appropriate judgment. Monitoring conditions over long periods, such as when determining anesthesia levels from electroencelophalogram (EEG), also place a considerable burden on physicians. Monitoring devices to automatically discriminate vascular conditions and accurately transmit information to physicians should be very useful.

No reports have, to our knowledge, been made on the development of diagnosis support based on vascular conditions, although studies exist on the estimation of vascular age [2,3]. Takada et al. [2] used acceleration plethysmogram by taking the second derivative of a plethysmogram and used statistics to determine its correlation with vascular age. This is not, however, quantitative nor can it be used for monitoring patients during surgery.

Vascular constriction is controlled by smooth muscles making up the arterial walls, and mechanical impedance is conventionally used to model the dynamic characteristics of muscles. Attempts have been made to quantify the dynamic characteristics of blood vessels using mechanical impedance, which consists of stiffness, viscosity, and inertia. Mussa-Ivaldi et al. [4] conducted one of the earliest studies of muscle impedance, in which they estimated hand stiffness with maintained arm posture. Tsuji et al. [5,6] succeeded to estimate stiffness and hand impedance components of viscosity and inertia by measuring impedance in different muscle contraction levels, postures, and directions of motion.

A few reports have modeled dynamic characteristics of the arterial wall using mechanical impedance. Mascaro and Asada [7] estimated impedance from information such as vascular diameter and blood flow velocity, although they do not detail their procedures and accuracy. Saeki et al. [8] quantitatively determined arterial wall compliance during surgery from changes in arterial pressure and plethysmogram. Applying estimation of skeletal muscle impedance [5], we proposed modeling arterial wall dynamics using the mechanical impedance of stiffness, viscosity, and inertia to estimate changing beat-to-beat conditions of blood vessels, and grasped vascular conditions in response to the physician's surgical actions as impedance changes [9].

In this paper, we estimated vascular conditions in which the scattering of estimation results due to individual differences is minimized by the use of impedance ratios, and attempted to identify vascular conditions from impedance ratio patterns. Many researchers have been reported the use of neural networks for pattern discrimination of biological signals [10-17]. Hiraiwa et al. [11,12] reported on discrimination of electrical potential patterns during voluntary movements, using an error back propagation

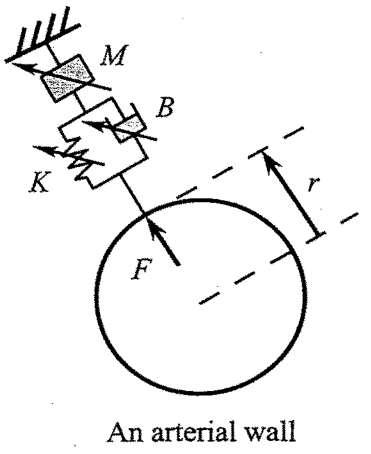

Fig. 1. Schematic description of the arterial wall impedance model considering only the characteristics in the arbitrary radius [9]. The vascular radius r and the force F caused by blood flow are measured to estimate the arterial wall impedance by using a second-order linear model.

neural network. Nishikawa et al. [13] conducted pattern discrimination from Gabor-transformed electromyogram (EMG) signals using an error back propagation neural network. As the complexity of the discrimination target increases, however, the number of training samples and training time for conventional error back propagation neural networks [14] increase, necessitating large neural networks. As one measure against this problem, Tsuji et al. proposed a log-linearized Gaussian mixture network (LLGMN), a type of feed-forward neural network. That uses a Gaussian mixture model for the network and acquires statistics by learning. Specifically, it has demonstrated superiority over other neural networks in the pattern discrimination of EMG [16,17].

This paper proposes using LLGMN to discriminate vascular conditions based on estimated biological signals such as arterial wall impedance and arterial pressure. Section 2 describes the vascular model and estimation for arterial wall impedance. Section 3 presents preliminary processing steps and discusses the characteristics of the neural network used for discriminating these conditions. Section 4 presents the results of experiments in vascular condition discrimination and discusses the feasibility of the proposed method.

2. Arterial Wall Impedance [9]

Figure 1 shows the impedance model for an arterial wall. Considering only characteristics of the arterial wall in an arbitrary radial direction, impedance characteristics can be expressed from radial force and wall displacement as follows:

$$F(t) = M\ddot{r}(t) + B\dot{r}(t) + K(r(t) - r_e) \quad . \; . \; . \; (1)$$

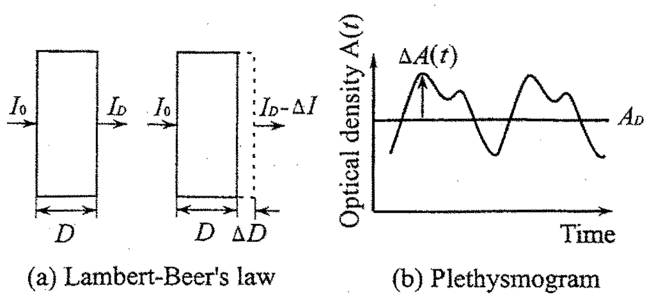

Fig. 2. Theory of plethsmogram

where $F(t)$ is the force exerted by blood flow on the arterial wall; M, B, and K are the inertia, viscosity, and stiffness; $r(t)$, $\dot{r}(t)$, and $\ddot{r}(t)$ are the position, velocity, and acceleration of the arterial wall; and r_e is the arterial radius without blood pressure acting. Using t_0 to denote the time when displacement starts, dynamic characteristics of the blood vessel at time t are expressed as follows:

$$dF(t) = Md\ddot{r}(t) + Bd\dot{r}(t) + Kdr(t) \quad . \; . \; . \; . \; . \; . \; (2)$$

where $dr(t) = r(t) - r(t_0)$, $d\dot{r}(t) = \dot{r}(t) - \dot{r}(t_0)$, $d\ddot{r}(t) = \ddot{r}(t) - \ddot{r}(t_0)$, and $dF(t) = F(t) - F(t_0)$.

$F(t)$ and $r(t)$ must be measured to estimate impedance parameters using (2). In this study, arterial pressure measurements are used to express $F(t)$. Assuming that arterial pressure is proportional to force, we have [9]:

$$F(t) = k_f P_b(t) \quad . \; . \; . \; . \; . \; . \; . \; . \; . \; . \; . \; . \; . \; . \; (3)$$

where k_f is a proportionality constant and $P_b(t)$ is arterial pressure.

Direct measurement of $r(t)$ is difficult to conduct invasively. So $r_v(t)$, which is the sum of all arterial radii at the measurement location, is estimated from plethysmogram.

Using I_0 to denote the intensity of LED-emitted incident light on a blood vessel of diameter D, and I_D to denote the intensity of transmitted light in **Fig.2(a)**, it follows from the Lambert-Beer's law [18] that:

$$A_D \equiv \log(I_0 / I_D) = ECD. \quad . \; . \; . \; . \; . \; . \; . \; . \; . \; (4)$$

where A_D is the absorbance due to an arterial diameter of D, shown to be proportional to density C of light absorbing material and arterial diameter D, and E is an absorbance constant unique to the material. Using $I_D - \Delta I(t)$ to denote the change in transmitted light caused by an arterial diameter change of D to $D + \Delta D(t)$, the change in absorbance $\Delta A(t)$ is given by (**Fig.2(b)**):

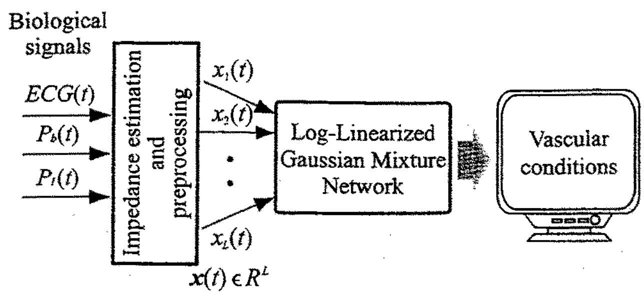

Fig. 3. Overview of vascular conditions discrimination based on the biological signals

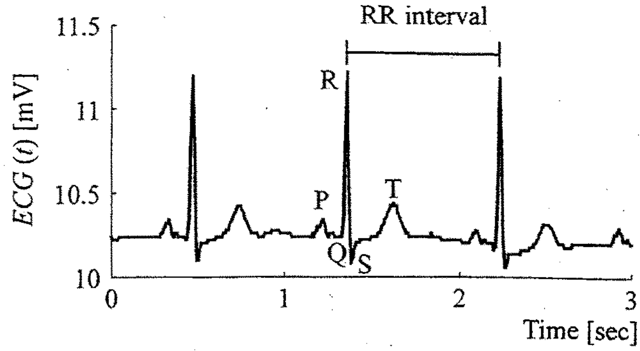

Fig. 4. Example of the measured electrocardiogram. The electrocardiogram consists of P wave, Q wave, R wave, S wave, and T wave in general.

$$\Delta A(t) = A(t) - A_D$$

$$= \log(I_D / (I_D - \Delta I(t))) = EC\Delta D(t) \quad . . . (5)$$

Plethysmogram $P_l(t)$ is a measure of $\Delta A(t)$.

Since plethysmogram varies in proportion to blood vessel pulsation, we simply assume that arterial radius is proportional to plethysmogram, which yields:

$$r_v(t) = \frac{P_l(t) + A_D}{k_p} \quad . . . . (6)$$

where $P_l(t)$ is the plethysmogram, k_p is a proportionality constant, and A_D is the absorbance.

Using arterial pressure $P_b(t)$ (of (3)) for force acting on the arterial wall and plethysmogram $P_l(t)$ (of (6)) for arterial radius, arterial wall impedance is estimated from the following equation:

$$dP_b(t) = \tilde{M} d\ddot{P}_l(t) + \tilde{B} d\dot{P}_l(t) + \tilde{K} dP_l(t) \quad . . . . (7)$$

where

$$\tilde{M} = \frac{M}{k_p k_f}, \tilde{B} = \frac{B}{k_p k_f}, \tilde{K} = \frac{K}{k_p k_f} \quad . . . . . (8)$$

and $dP_b(t) = P_b(t) - P_b(t_0)$, $dP_l(t) = P_l(t) - P_l(t_0)$. Here, $\tilde{M}$ is viewed as representing mass and $\tilde{B}$ and $\tilde{K}$ viscous and elastic characteristics of the arterial wall.

3. Discrimination of Vascular Conditions Using a Neural Network

Figure 3 shows vascular condition discrimination using a neural network. This section details preliminary processing and the LLGMN [5] used to discriminate vascular conditions.

3.1. Preliminary Processing

Figure 4 shows an example of the measured ECG signal. The P wave corresponds to atrial excitation, the QRS wave to ventricular excitation, and the T wave to ventricular repolarization [19]. The R wave generally has a distinctly large amplitude, and so is used in this study to mark ECG signal divisions. Defining the time when the R wave appears in each ECG recognition cycle as t_0, arterial pressure $dP_b(t)$ and plethysmogram $dP_l(t)$ for the interval (RR interval) between the R wave and the subsequent R wave are used to determine impedance parameters of (8) by the method of least squares. Since the previous RR interval is established each time an R wave is detected, it is possible to estimate beat-to-beat arterial wall impedance parameters $\tilde{M}$, $\tilde{B}$ and $\tilde{K}$. Proportionality factors k_f and k_p in (8) are unknown parameters that vary with each subject, and give rise to individual differences. Because input parameters that carry considerable individual differences make it difficult to conduct pattern discrimination with neural networks, a preliminary process is done to minimize the effect of individual differences.

In this paper, the preliminary process involves computation of ratios. Impedance ratios $\tilde{M}_{ratio}$, $\tilde{B}_{ratio}$, and $\tilde{K}_{ratio}$ of $\tilde{M}$, $\tilde{B}$, and $\tilde{K}$ in (8), relative to impedance parameters $\tilde{M}_{rest}$, $\tilde{B}_{rest}$, and $\tilde{K}_{rest}$ when the vascular condition is relatively stable, are calculated by the following equations:

$$\tilde{M}_{ratio} = \frac{\tilde{M}}{\tilde{M}_{rest}}, \tilde{B}_{ratio} = \frac{\tilde{B}}{\tilde{B}_{rest}}, \tilde{K}_{ratio} = \frac{\tilde{K}}{\tilde{K}_{rest}} \quad . . (9)$$

Similarly, ratios of arterial pressure and plethysmogram also are calculated to minimize the effects of individual differences in biological signals as follows:

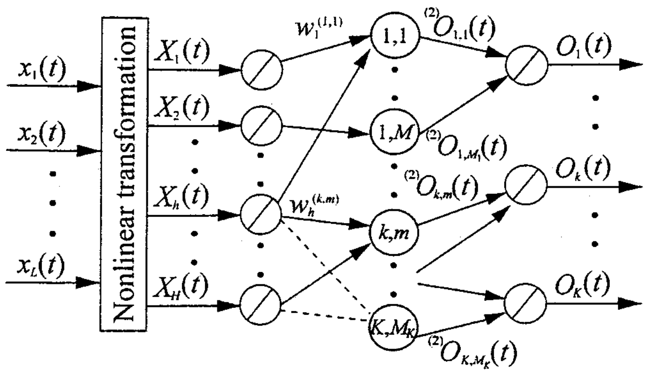

Fig. 5. Structure of LLGMN

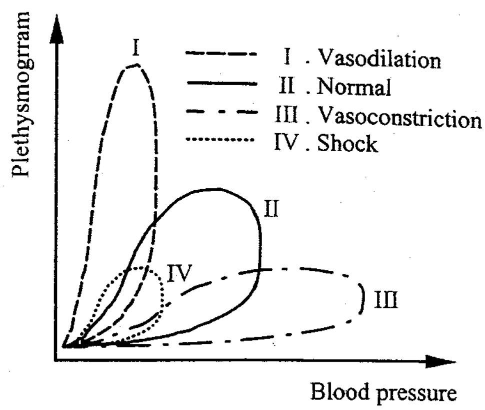

Fig. 6. Biological signals and vascular conditions

$$IBP_{\text{ratio}} = \frac{IBP_{\max} - IBP_{\min}}{IBP_{\text{rest}}} \quad \cdots\cdots\cdots (10)$$

$$PLS_{\text{ratio}} = \frac{PLS_{\max} - PLS_{\min}}{PLS_{\text{rest}}} \quad \cdots\cdots\cdots (11)$$

where $IBP_{\max}$, $IBP_{\min}$, $PLS_{\max}$, and $PLS_{\min}$ are maximum and minimum arterial pressure and plethysmogram during each beat-to-beat interval. IBP_{rest} and PLS_{rest} are differences between maximum and minimum arterial pressure and plethysmogram in a relatively rested condition.

Impedance ratios and biological signal ratios defined by (9)–(11) are input to the neural network as characteristic vector $x(t) = [x_1(t), x_2(t), \cdots, x_L(t)]^{\mathrm{T}} \in \Re^L$ $(L=5)$.

3.2. Neural Network

The LLGMN [15] is shown in **Fig.5**. Input vector $x(t)$ at time t is first subjected to nonlinear transformation as follows:

$$X(t) = [1, x(t)^T, x_1(t)^2, x_1(t)x_2(t), \cdots,$$
$$x_1(t)x_L(t), x_2(t)^2, x_2(t)x_3(t),$$
$$\cdots, x_2(t)x_L(t), \cdots, x_L(t)^2]^{\mathrm{T}} \quad \cdots (12)$$

This transformation is done to represent normal distributions of each component of the Gaussian mixture model in linear computation of new input vector $X(t)$ and neural network's weight coefficients.

The neural network's first layer consists of H units in agreement with the number of dimensions $H = 1 + L(L+3)/2$ of $X(t)$. Each unit uses an identity function for input-output functions, so input $X_h(t)$ comes out as the output. Weights $w_h^{(k,m)}$ are applied to the first layer's outputs, which are then sent to the second layer.

Using $^{(1)}O_h(t)$ to denote the first layer's output, inputs to and output from unit $\{k,m\}$ of the second layer, denoted by $^{(2)}I_{k,m}(t)$ and $^{(2)}O_{k,m}(t)$, are given by:

$$^{(2)}I_{k,m}(t) = \sum_{h=1}^{H} {}^{(1)}O_h(t) w_h^{(k,m)} \quad \cdots\cdots\cdots (13)$$

$$^{(2)}O_{k,m}(t) = \frac{\exp[^{(2)}I_{k,m}(t)]}{\sum_{k'=1}^{K}\sum_{m'=1}^{M_{k'}} \exp[^{(2)}I_{k',m'}(t)]} \quad \cdots\cdots (14)$$

where $w_k^{(K,M_K)}$ $(h = 1, 2, \cdots, H)$, with $k = 1, 2, \cdots, K$ and $m = 1, 2, \cdots, M_k$. K represents the vascular conditions, and M_k the number of components of Gaussian distribution belonging to vascular condition k. Unit k of the third layer is linked to M_k units of the second layer, given by the following input-output relation:

$$^{(3)}I_k(t) = \sum_{m=1}^{M_k} {}^{(2)}O_{k,m}(t) \quad \cdots\cdots\cdots (15)$$

$$^{(3)}O_k(t) = {}^{(3)}I_k(t) \quad \cdots\cdots\cdots (16)$$

Outputs of the third layer units give posterior probabilities of vascular conditions. The vascular condition with the highest probability is considered most likely at time t.

Learning of the neural network is as follows: The LLGMN learns to maximize the logarithmic likelihood based on N data samples $x(n)$ $(n = 1, \cdots, N)$. Consider the case when training vector $T(n) = [T_1(n), T_2(n), \cdots, T_K(n)]^{\mathrm{T}}$ is given for nth input vector $x(n)$. $T_k(n)$ is unity for event k, otherwise zero. Since LLGMN output $O_k(n)$ corresponds to posterior probabilities, learning takes place by minimizing evaluation function J given by [15]:

$$J = -\sum_{n=1}^{N}\sum_{k=1}^{K} T_k(n) \log O_k(n) \quad \cdots\cdots\cdots (17)$$

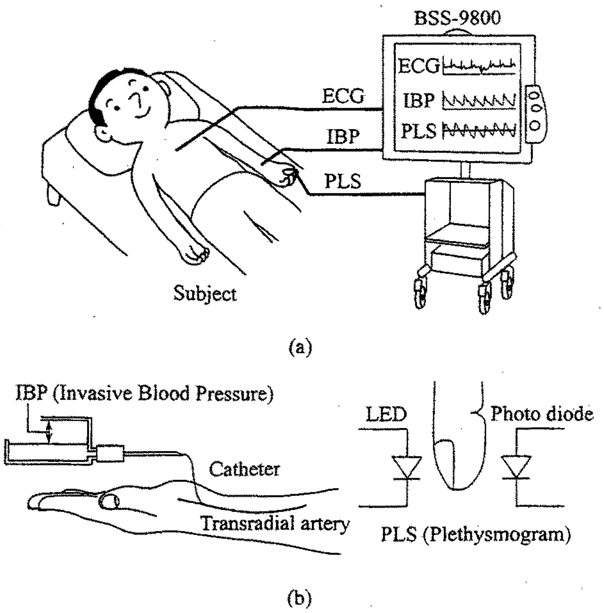

Fig. 7. (a) Experimental apparatus. **(b)** IBP is measured at transradial artery of wrist using a catheter, and PLS is measured with the ipsilateral thumb.

3.3. Discrimination Rule

A discrimination error occurred in the vascular condition prevents proper treatment and gives rise to serious consequences from misdiagnosis. To avoid such errors, the neural network should not conduct discrimination of information that consists of signals containing noise. The coefficient of determination of the arterial wall impedance model given by (7) is thus used for judging whether discrimination should take place. The coefficient of determination is used to evaluate how successful parameter estimation was [9].

First, the coefficient of determination is determined from measured arterial pressure and arterial pressure calculated from impedance estimation based on (7) [20]. Then, the coefficient of determination R^2 is compared to threshold R_d^2 to determine whether to suspend discrimination. If $R^2 \geq R_d^2$, the discrimination result is adopted as the vascular condition; if $R^2 < R_d^2$, then discrimination is withheld since the received signal is inappropriate.

3.4. Vascular Conditions

Vascular conditions targeted for discrimination were defined on the basis of Lissajous's figures in **Fig.6** [8]. The abscissa represents the arterial pressure, and the ordinate plethysmogram values, so figures provide a rough diagnosis of vascular conditions. The following four conditions were set up for discrimination:

I. **Vasodilation:** It is the process by which blood vessels are dilated in the extremities (arms and legs), allowing a greater volume of blood to flow to these tissues.

II. **Normal:** Normal condition in which blood circulation is stable.

III. **Vasoconstriction:** It decreases the diameter of the vessel lumen to allow less blood through. This is caused by the dilation or contraction of the smooth muscle in the vessel walls, particularly in the arterioles. It is the exact opposite to the vasodilation.

IV. **Shock:** A condition due to inadequate blood supply to tissues which is life-threatening.

It is possible to refine settings with sufficient learning signals. Determination of the optimal number of setting levels is planned in projected investigation.

4. Discrimination Experiment

4.1. Experimental Condition

A discrimination experiment was conducted to verify the feasibility of the proposed method. The apparatus measuring biological signals used for estimation is shown in **Fig.7**. The two subjects consisted were one undergoing endoscopic transthoracic sympathectomy (patient A) and the other a partial resection of the tongue cancer (patient B). Endoscopic transthoracic sympathectomy is taken against hyperhidrosis, in which hyperfunction of sympathetic nerves in the thorax causes excessive sweating in the palms or underarm, and which is usually accompanied by blood vessel constriction. Sympathetic nerves are interrupted with a clip to stop local sweating [21]. Such surgery dilates blood vessels, so our proposed method may enable monitoring the success or failure of surgery. Partial resection of the tongue cancer was undertaken to remove a cancer tumor.

ECG, arterial pressure, and plethysmogram were simultaneously measured during surgery to discriminate vascular conditions. A bedside monitor (BSS-9800, Nihon Kohden Corp.) was used for measurement, with data stored in a personal computer at a sampling frequency of 125 Hz. Arterial pressure was measured by inserting a catheter in the left radial artery. Plethysmography was measured using the thumb on the same side.

Neural network learning signals were obtained from four patients other than subjects A and B, who underwent endoscopic transthoracic sympathectomy. However, we were unable to obtain learning signals corresponding to the defined vascular conditions of "vasodilation" and "shock." Missing data were thus generated from normalized random numbers $N(\mu, 0.1)$. In this paper, the means μ was set as follows: $\mu_{IBP_{ratio}} = 0.5$, $\mu_{PLS_{ratio}} = 1.5$, $\mu_{\tilde{M}_{ratio}} = 0.33$, $\mu_{\tilde{B}_{ratio}} = 0.33$, and $\mu_{\tilde{K}_{ratio}} = 0.33$ for vasodilation; $\mu_{IBP_{ratio}} = 0.2$, $\mu_{PLS_{ratio}} = 0.2$, $\mu_{\tilde{M}_{ratio}} = 1.0$, $\mu_{\tilde{B}_{ratio}} = 1.0$, and $\mu_{\tilde{K}_{ratio}} = 1.0$ for shock.

4.2. Discrimination Results

Discrimination results using the LLGMN are shown

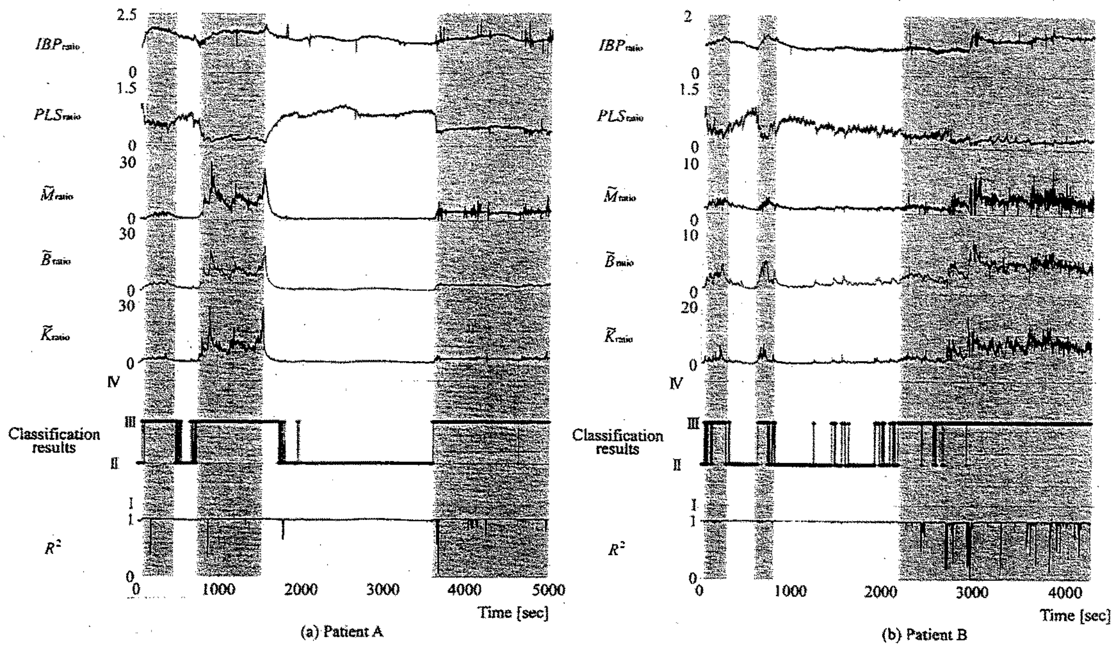

Fig. 8. Classification results of the vascular conditions during surgical operations

in **Fig.8**. In order from the top, plots represent the arterial pressure variation ratio, plethysmogram variation ratio, inertia ratio, viscosity ratio, stiffness ratio, the vascular condition discrimination results, and coefficient of determination. Shaded regions indicate vasoconstriction conditions. Ten data samples were obtained immediately before surgery, when the patient was sufficiently anesthesthetized and sample means were used as reference (rest) values. A threshold of $R_d^2 = 0.9$ was adopted for the present case, below which discrimination was withheld and the previous discrimination result maintained.

In results for patient A (**Fig.8(a)**), the physician searches for the sympathetic nerve to be interrupted during 700–1,500 sec. Sympathetic nerves are excited, causing blood vessels to constrict and impedance parameters to increase. The neural network discriminated vasoconstriction. After the sympathetic nerve was interrupted at around 1,500 sec, a normal, stable condition is discriminated. After 3,700 sec, anesthesia wears off so blood vessels constrict, once again discriminated as a state of vasoconstriction. Results show that arterial wall impedance and biological signals are successful in discriminating vascular conditions arising from the physician's surgical actions and the patient's condition.

Patient B underwent surgery accompanied by severe pain during 100–800 sec, and anesthesia began to wear off after 2,200 sec. As in the previous subject, all impedance parameters increase during vasoconstriction, with successful discrimination. Due to noise, discrimination of conditions is unstable at times such as when anesthesia begins to wear off, suggesting that future investigations should include the determination of an optimal setting for the coefficient of determination threshold. Even so, overall vascular conditions were discriminated successfully with patients undergoing different surgery, demonstrating the feasibility of the proposed method.

5. Conclusions

This paper discussed neural-network-based discrimination of vascular conditions, targeting development of a diagnosis support system for conveying information the physician needs to understand the patient's vascular conditions. When the method was used in discrimination experiments using data measured during actual surgery, vascular conditions corresponding to the physician's surgical actions were successfully discriminated, thus demonstrating the feasibility of the proposed method.

Future research will include improvement of the discrimination rate and testing the method's validity using different surgery data. We also plan to develop monitoring based on real-time discrimination for use in actual surgery.

Acknowledgements
We thank Mr. Teiji Ukawa and Mr. Katsuhide Tone, Nihon Kohden Corporation, for their kind assistance. This study was supported in part by a Grant-in-Aid for Scientific Research (15008279) from the Japan Society for the Promotion of Science, to which the authors express their thanks.

References:
[1] D.E.Longnecker and F.L.Murphy, "Introduction to Anesthesia", Elsevier Science Health Science div, 1997.
[2] H.Takada, S.M.Mirbod, and H.Iwata, "The relative vascular age

derived from acceleration plethysmogram: A new attempt," Jpn. J. Appl. Physiol., Vol. 28, No. 2, pp. 115-121, 1998.
[3] Y.Maniwa, T.Iokibe, M.Koyama, M.Yamamoto, and S.Ohta, "The Application of Pulse Wave Chaos in Clinical Medicine," in Proc. 17th FUZY System Symposium, Chiba, pp. 787-790, 2001.
[4] F.A.Mussa-Ivaldi, N.Hogan, and E.Bizzi, "Neural, mechanical and geometrical factors sub-serving arm posture in humans," Journal of Neuroscience, Vol. 5, No. 10, pp. 2732-2743, 1985.
[5] T.Tsuji, P.G.Morasso, K.Goto, and K.Ito, "Human hand impedance characteristics during maintained posture," Biol. cybern., Vol. 72, No.6 pp. 475-485, 1995.
[6] T.Tsuji and M.Kaneko, "Estimation and Modeling of Human Hand Impedance during Isometric Muscle Contraction," in Proc. ASME., DSC-Vol. 58, pp. 575-582, Atlanta, 1996.
[7] A.Mascaro, and H.Asada, "Photoplethysmograph Fingernail Sensors for Measuring Finger Forces Without Haptic Obstruction," IEEE Trans. Robot. Automat., Vol. 17, No. 5, pp. 698-708, 2001.
[8] N.Saeki, M.Kawamoto, and O.Yuge, "Quantitative view of peripheral circulation," Critical Care Medicine, Vol. 28, No. 12, A62(suppl), 2000.
[9] A.Sakane, T.Tsuji, Y.Tanaka, N.Saeki, and M.Kawamoto, "Estimating Arterial Wall Impedance using a Plethysmogram," in Proc. 29th Annual Conference of the IEEE Industrial Electronics Society, pp. 580-585, USA, 2003.
[10] M.Peltoranta and G.Pfurtscheller, "Neural network based classification of non-averabed event-related EEG responses," Med and Biol. Eng. and Comput., Vol. 32, pp. 189-196, 1994.
[11] A.Hiraiwa, K.Shimohara, and Y.Tokunaga, "EMG pattern analysis and classification by neural network," in Proc. IEEE International Conference on Syst., Man and Cybern., pp. 1113-1115, 1989.
[12] A.Hiraiwa, U.Uchida and K.Shimohara, "EMG/EEG pattern recognition by neural networks," in Proc. Eleventh European Meeting on Cybernetics and Systems Research, pp. 1383-1390, 1992.
[13] D.Nishikawa, W.Yu, H.Yokoi, and Y.Kuhazu, "EMG Prosthetic Hand Controller Discriminating Ten Motions using Real-time Learning Method," in Proc. 1999 IEEE/RSJ International Conference on Intelligent Robotics and Systems, pp. 1592-1597, 1999.
[14] D.D.Rumelhart, G.E.Hinton, and R.J.Williams, "Learning internal representations by error propagation," in Parallel Distributed Processing I, pp. 318-362, MIT Press, 1986.
[15] T.Tsuji, H.Ichinobe, and M.Kaneko, "A Proposal of the Feedforward Neural Network Based on the Gaussian Mixture Model and the Log-Linear Model," Trans. Institute of Electronics, Information and Communication Engineers, Vol. J77-D-II, No. 10, pp. 2093-2100, 1994 (in Japanese).
[16] T.Tsuji, O.Fukuda, H.Ichinobe, and M.Kaneko, "A Log-Linearized Gassian Mixture Network and Its Application to EEG Pattern Classification," IEEE Trans. Syst., Man, Cybern-Part C, Appl. and Rev., Vol. 29, No. 1, pp. 60-72, 1999.
[17] T.Tsuji, O.Fukuda, M.Murakami, and M.Kaneko, "An EMG Controlled Pointing Device Using a Neural Network," Trans. of the Society of Instrument and Control Engineers, Vol. 37, No. 5, pp. 425-431, 2001 (in Japanese).
[18] R.A.Day and A.L.Underwood, QUANTITATIVE ANALYSIS 4th Edition. Prentice-Hall, 1980.
[19] N.Goldschlager and M.J.Goldman, Principles of Clinical Electrocardiography, Prentice Hall, 1989.
[20] J.Archdeacon, Correlation and Regression Analysis, Univ of Wisconsin Pr., 1994.
[21] C.Drott, G.Gothberg, and G.Claes, "Endoscopic transthoracic sympathectomy: An efficient and safe method for the treatment of hyperhidrosis," Journal of the American Academy of Dermatology, Vol. 33, pp. 78-81, 1995.

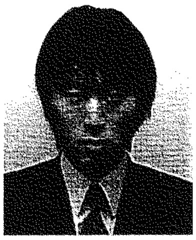

Name:
Akira Sakane

Affiliation:
Department of Artificial Complex Systems Engineering, Hiroshima University

Address:
1-4-1 Kagamiyama, Higashi-Hiroshima, Hiroshima 739-8527, Japan

Brief Biographical History:
1999- Faculty of Engineering, Hiroshima University
2001- Master Course, Graduate school of Engineering, Hiroshima University
2003- Doctor Course, Graduate school of Engineering, Hiroshima University
2003- Research Fellow of Japan Society for the Promotion of Science (JSPS)

Main Works:
- "Estimating Arterial Wall Impedance using a Plethysmogram," in Proc. 29th Annual Conference of the IEEE Industrial Electronics Society, pp. 580-585, USA, 2003.
- "Bio-mimetic Control of Mobile Robots Based on a Model of Bacterial Chemotaxis," Trans. Jpn. Soc. Mech. Eng., Vol. 68, No. 673, C, pp. 2687-2694, 2002.

Membership in Learned Societies:
- The Institute of Electrical and Electronics Engineers (IEEE)
- The Japanese Society of Instrumentation and Control Engineers (SICE)
- The Society of Biomechanisms Japan (SOBIM)

Name:
Toshio Tsuji

Affiliation:
Department of Artificial Complex Systems Engineering, Hiroshima University

Address:
1-4-1 Kagamiyama, Higashi-Hiroshima, Hiroshima 739-8527, Japan

Brief Biographical History:
1985- Research Associate at Hiroshima University
1994- Associate Professor at Hiroshima University
2002- Full Professor at Hiroshima University

Main Works:
- "A Recurrent Log-linearized Gaussian Mixture Network," IEEE Trans. Neural Networks, Vol. 14, No. 2, pp. 304-316, 2003.

Membership in Learned Societies:
- The Institute of Electrical and Electronics Engineers (IEEE)
- The Robotics Society of Japan (RSJ)
- The Japanese Society of Instrumentation and Control Engineers (SICE)

Name:
Noboru Saeki

Affiliation:
Department of Anesthesiology and Critical Care, Graduate School of Biomedical Sciences, Hiroshima University

Address:
1-2-3 Kasumi, Minami-ku, Hiroshima 734-8551, Japan

Brief Biographical History:

1995- Doctor Course, Graduate School of Medicine, Hiroshima University

2000- Research Associate, Graduate School of Medicine, Hiroshima University

Main Works:

- "Albumin Permeability Across Endothelial Cell Monolayer Exposed to Reactive Oxygen Inter mediates: Involvement of Reversible Functional Alteration of the Cell Membrane Ca^{2+} Channels," Hiroshima Journal of Medical Sciences, ~~Vol. 49, No.~~ 1, pp. 57-65, 2000.
- "Quantitative view of peripheral circulation," Critical Care Medicine, Vol. 28, No. 12, A62(suppl), 2000.

Membership in Learned Societies:

- The Japanese Society of Anesthesiologists (JSA)
- The Japan Society for Clinical Anesthesia (JSCA)

Name:
Masashi Kawamoto

Affiliation:
Department of Anesthesiology and Critical Care, Graduate School of Biomedical Sciences, Hiroshima University

Address:
1-2-3 Kasumi, Minami-ku, Hiroshima 734-8551, Japan

Brief Biographical History:

1979- Instructor, Hiroshima University School of Medicine

1990- Associate Professor, Miyazaki Medical College

1992- Associate Professor, Graduate School of Medicine, Hiroshima University

Main Works:

- "Effect of JTC-801 (nociceptin antagonist) on neuropathic pain in a rat model," Neuroscience Letters, Vol. 351, No. 3, pp. 133-136, 2003.
- "Heart rate to arterial pressure impulse response during one lung ventilation," Acta Anaesthesiologica Scandinavica, Vol. 46, No. 5, pp. 592-598, 2002.

Membership in Learned Societies:

- The Japanese Society of Anesthesiologists (JSA)
- The American Society of Anesthesiologists (ASA)
- The Society of Critical Care Medicine (SCCM)